PAPER

Check for updates

Bidirectional ROMP of paracylophane-1,9-dienes to tri- and penta-block *p*-phenylenevinylene copolymers†

Venukrishnan Komanduri, [ID] Dharam R. Kumar, Daniel J. Tate, [ID] Raymundo Marcial-Hernandez, Benjamin J. Lidster and Michael L. Turner [ID] *

Dialkoxy and dialkyl substituted paracyclophane-1,9-dienes undergo bidirectional ring opening metathesis polymerisation (ROMP) on addition of bifunctional Hoveyda–Grubbs initiators. The living nature of the polymerisation was demonstrated for different [monomer]/[initiator] ratios and block copolymers were prepared by sequential ROMP and ROMP-ATRP to give fully conjugated rod–rod–rod and partially conjugated coil–rod–coil ABA and BAB triblock copolymers, respectively. These strategies were successfully extended to the synthesis of the corresponding pentablock copolymers. Optical and electrochemical properties of *cis/trans* and all *trans* homo and block copolymers are discussed.

Introduction

π-Conjugated polymers have found extensive application as active layers in the fabrication of optoelectronic and electronic devices such as OLEDs,[1] OFETs,[2,3] OPVs[4,5] and sensors.[6,7] Key advantages for the use of polymeric materials include improved flexibility, mechanical robustness, lighter weight and ease of processing.[8] The performance of these devices is greatly influenced by the morphology of the active layer, and this is strongly influenced by the kinetics of thin film formation during device fabrication. An attractive approach to obtaining reproducible thin film morphologies is to utilise the thermodynamically driven phase separation of block copolymers, as these materials form well defined nanostructures that can be self-assembled in biphasic media.[9,10] Block copolymers with conjugated segments can either be fully conjugated rod–rod systems, in a diblock or rod–coil systems where the conjugated block is coupled to a saturated polymer backbone.[11] There are only a few polymerisation methods that give well-defined fully conjugated block copolymers. These include Kumada catalyst-transfer polymerisation (KCTP also known as GRIM),[12,13] a nickel catalysed Negishi type polymerisation[14] and a palladium catalyst transfer Suzuki–Miyaura polycondensation.[15] The synthesis of rod–coil systems has been more extensively reported, including the ROMP of cyclooctadiene

followed by ATRP of the resulting macroinitiator.[16] Phenylenevinylene (PPV) block copolymers can be prepared by the Siegrist polycondensation or by complex multistep syntheses.[17,18,18] However these approaches lead to poor control of the molecular weight distribution and result in polymers with broad polydispersities (Đ_m) and significant backbone defects.[19]

Ring opening metathesis polymerisation (ROMP) of strained paracyclophanedienes[20–24,25] and cyclophane-trienes[26,27] gives well-defined PPV homopolymers and fully conjugated diblock copolymers.[28,29] Rod-coil PPV diblock copolymers can be prepared by the sequential one-pot ROMP of tetraalkoxy paracyclophanediene and oxanorbornene monomers.[30] This sequential ROMP strategy was adopted by Weck *et al.* using di, tetraalkoxy cyclophanedienes and norbornene ester monomers to access PPV tri and tetrablock copolymers.[31,32] A step-wise strategy using monotelechelic PPV blocks as macroinitiators for ATRP of methylmethacrylate gives rod–coil PPV-PMMA diblock copolymers.[33] Rod–coil PPV block copolymers have also been prepared through the preparation of PPV macroinitiators using anionic polymerisation followed by the introduction of the coil unit using a radical polymerisation.[34] However, to date there have been very few reports on the preparation of fully and partially conjugated PPV triblock copolymers. These include an ADMET polymerisation/ Wittig olefination strategy to prepare fully conjuagted ABA and ABCBA type PPV block copolymers[35] and the synthesis of donor–acceptor–donor triblock copolymers by a Knoevenagel condensation followed by a Nickel catalysed Yamamoto coupling by Tu *et al.*[36] Coil–rod–coil ABA triblock copolymers with pendent PEG chains have been prepared by a Heck coupling

Organic Materials Innovation Centre (OMIC), The School of Chemistry, The University of Manchester, Oxford Road, Manchester, M13 9PL, UK. E-mail: michael.turner@manchester.ac.uk

†Electronic supplementary information (ESI) available. See DOI: 10.1039/ c9py00147f

strategy[37] and ferrocene containing ABC triblock copolymers have been made by an anionic polymerisation-Wittig olefination approach.[38] These strategies all involve complex multistep syntheses and lead to poor control over the molecular weight distribution.

In this study we report a precisely controlled approach to the synthesis of conjugated triblock copolymers,[23] by the ROMP of cyclophanediene monomers **M1** and **M2** with bifunctional ruthenium complex **1** to form the telechelic polymer intermediate [**I**] (Fig. 1). Trapping of this intermediate with a second cyclophanediene gives the fully conjugated rod–rod–rod ABA triblock copolymer. Quenching of the intermediate [**I**] with an α-bromoester functionalised vinylether **E** followed by ATRP of the resulting macroinitiator generates coil–rod–coil ABA triblock copolymers. This approach can be extended to the synthesis of the corresponding pentablock copolymers. To our knowledge this is the first bidirectional ROMP[39] of paracyclophanedienes using bifunctional ruthenium carbene initiators towards the synthesis of conjugated multiblock copolymers (Fig. 1).

Results and discussion

Initial optimisation studies focussed on the ROMP of monomers **M1** and **M2** using the bifunctional catalyst **1**. The required cyclophane-1,9-diene monomers **M1** (R = *O*-2-ethylhexyl)[33] and **M2** (R = *n*-octyl)[40] were prepared using standard synthetic procedures. The bifunctional catalyst **1** was synthesised by cross metathesis of Grubbs second generation catalyst **G2** with 2,5-dimethoxy-1,4-divinylbenzene as reported.[41]

The first ROMP experiment was performed using dialkoxy monomer **M1** ([**M1**]/[**1**] = 10) in DCM-d_2 at room temperature. The polymerisation was followed by *in situ* ^{1}H NMR spectroscopy and complete monomer consumption was observed after 63 h. However, reaction times were reduced to 10 h when the ROMP was performed at 60 °C in TCE-d_2 (Fig. S3†). After consumption of the monomer the polymerisation was quenched with excess ethylvinylether and stirred at rt for 4 h. Precipitation of the crude product (MeOH/Celite), followed by elution with chloroform gave telechelic PPV **2a** ($M_{n(calc.)}$ = 4.7 kDa, $M_{n(obs)}$ = 5.7 kDa, $Đ_m$ = 1.40) in 95% yield (entries 1 and 2, Table S1†).

Bidirectional ROMP of the dialkyl monomer **M2** ([**M2**]/[**1**] = 10) in DCM-d_2 at room temperature was complete in 1.5 h but gave poor control over the molecular weight distribution ($M_{n(calc.)}$ = 4.4 kDa, $M_{n(obs)}$ = 79 kDa, $Đ_m$ = 1.8) due to incomplete initiation and fast propagation. The higher propagation rates are due to the absence of Lewis basic sites in monomer **M2** that can ligate to the intermediate 14 electron ruthenium complex formed after initiation. Therefore, the ROMP was performed in the presence of an external ligand 3-BrPy (40 mol%) at 40 °C in TCE-d_2 for 20 h (Fig. S4†) to slow down propagation. This gave PPV **3a** with significant control over molecular weight ($M_{n(obs)}$ ∼ 7.1 kDa *vs.* 79 kDa in the absence of 3-BrPy, entries 3 and 4, Table S1†). Further control over the molecular weight and an improved yield was obtained ($M_{n(obs)}$ ∼ 5.4 kDa) when the ROMP was performed at 40 °C using anhydrous degassed DCM as solvent (entries 4 and 5, Table S2†). This could be due to the better solubility of **1** in DCM. The living nature of the polymerisation was demonstrated by varying the [monomer]/[initiator] ratio to obtain polymers **2a–c** (96–93% yield) and **3a–c** (95–81% yield) as shown in Fig. 2 (also, see Table S2†). The [**M**]/[**I**] ratios given for the monomers **M1** and **M2** are different because ROMP of **M1** under the optimal conditions gives poor control of the molecular weight and dispersity beyond ratios of 20 : 1.

A powerful application of this bidirectional ROMP methodology was demonstrated by the synthesis of both rod–rod–rod and coil–rod–coil triblock copolymers. Triblock conjugated copolymers have found interesting application as the active layer in OPV and OLED devices[42] but only limited synthetic
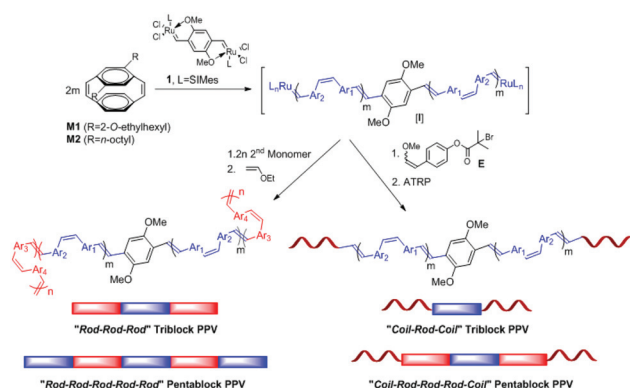

Fig. 1 A bidirectional ROMP of strained paracyclophanediene monomers to both partially and fully conjugated tri and pentablock copolymers.
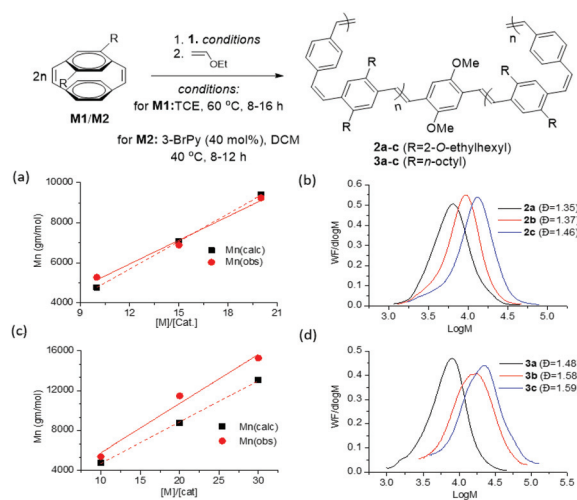

Fig. 2 Bidirectional ROMP of monomers **M1** and **M2** with initiator **1**. (a) and (c) dependence of M_n of the polymers **2a–c** and **3a–c** on [**M**]/[**1**] ratio, (b) and (d) molecular weight distribution of polymers **2a–c** and **3a–c** respectively.

methods have been reported. AB and ABA block copolymers with PPV units are known to self-assemble into nano-structures, the morphology of which depends on the mole fraction of the individual blocks.[9,43]

The α-bromoester end capped PPV macroinitaitors **4a** and **5a** were prepared in excellent yields (95–98%) by bidirectional ROMP of monomers **M1** and **M2** followed by quenching with α-bromoester phenyl methylvinyl ether **E** (f = 89% and 75%, see Table S2†). Matrix-assisted laser desorption/ionization time-of-flight mass spectrometry (MALDI-TOF-MS) of polymer **4a** and **5a** showed major peaks corresponding to the desired polymers with α-bromoester end groups (●), the major series of peaks separated by the mass of the polymer repeat unit 461.4 Da and 428.9 Da corresponding to the molecular weights of monomers **M1** and **M2** respectively (Fig. 3, S19†).[44]

These macroinitiators (**4a** and **5a**) were subjected to CuBr mediated atom transfer radical polymerisation (ATRP)[33] with methyl methacrylate (MMA) in hot toluene for 3 h. Aliquots of the reactions were terminated at different time intervals (30, 90, 180 min) by exposing to air followed by precipitation into excess methanol. The solids were redissolved in chloroform and precipitated by addition of diethyl ether. Upon filtration, PMMA-*b*-PPV-*b*-PMMA triblock polymers **6a–c** and **7a–c** were obtained as orange/yellow solids with dispersities ranging from 1.23 to 1.33 and a unimodal molar mass distribution by GPC analysis (Scheme 1, Fig. S21 and Table S3†).

The MMA content in these triblock copolymers was determined from the ^{1}H NMR spectra by a comparison of the integration of the OMe group of MMA (δ = 3.98–3.17 ppm) against the combined phenyl and vinylene protons for **6a–c** (δ = 7.93–6.34 ppm) and methylene protons for **7a–c** (δ = 2.86–2.16 ppm) respectively (Fig. S22–27, Table S3†).

Bidirectional living polymerisation of cyclophanedienes in a sequential manner gave fully conjugated triblock copolymers. ROMP of monomer **M1** with initiator **1** ([**M1**]/[**1**] = 10) in TCE at 60 °C was monitored by GPC and TLC analyses (Fig. S47†). After complete consumption (t = 8 h) of monomer **M1** an external ligand, 3-BrPy (40 mol%), and a solution of the second monomer **M2** in TCE were added. The reaction mixture was stirred at 40 °C until the second monomer **M2** was consumed (t = 12, 16 and 18 h) and the polymerisation was quenched with excess ethylvinylether. Purification by precipitation (Celite/MeOH) and elution with chloroform afforded fully conjugated ABA triblock polymers **8a–c** in 80–88% yields
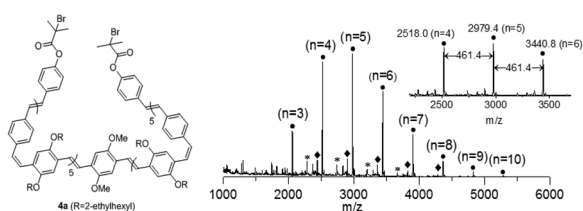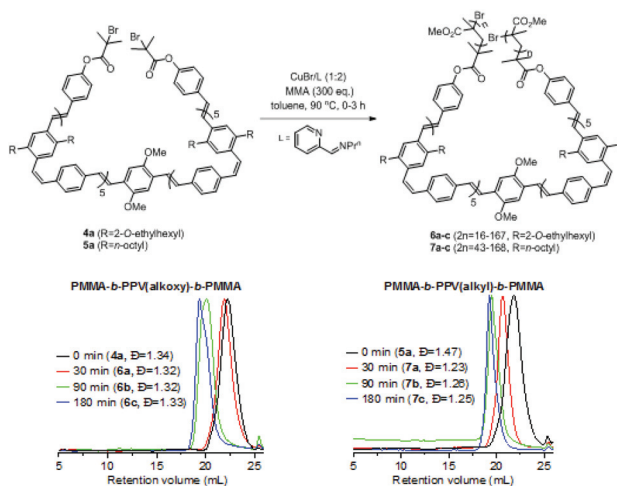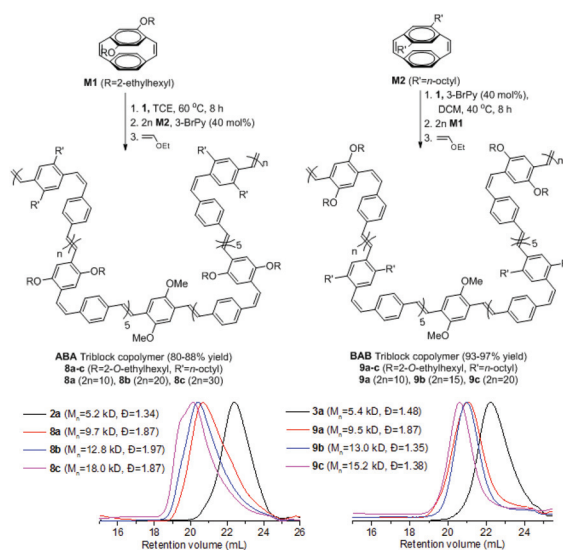

Scheme 1   ROMP-ATRP strategy to prepare coil–rod–coil ABA phenylenevinylene triblock copolymers **6a–c** and **7a–c** (GPC in THF).

with dispersities ranging from 1.87–1.97. The higher polydispersities and the shoulder peak observed in the GPC traces of block copolymer **8c** can be assigned to partial isomerisation of the *cis*-alkenes (Scheme 2, left and Table S4†). The sequential ROMP strategy was more efficient (yields 93–97% and $Đ_m$ = 1.35–1.87) when the monomer addition sequence was reversed to give BAB triblock copolymers **9a–c** containing alkyl PPV segments at the center and alkoxy PPV units on either side (Fig. S48,† Scheme 2, right and Table S4†).

The triblock copolymers **8a–c** and **9a–c** were characterised by ^{1}H NMR spectroscopy and the ratio of monomer units **M1** and **M2** incorporated was calculated by combined integration of the alkoxy methylene protons corresponding to **M1** and the methoxy protons of **1** (δ 4.12–3.77 ppm) against the benzyl

Fig. 3   MALDI-TOF-MS of macroinitiator **4a** (●) peaks correspond to α-bromoester end groups (✳) phenol with elimination of HBr and (✦) PPV with elimination of HBr.

Scheme 2   Sequential ROMP strategy to fully conjugated rod–rod–rod ABA (**8a–c**) and BAB (**9a–c**) phenylenevinylene triblock copolymers (GPC in THF).

protons corresponding to **M2** (δ 2.72–2.20 ppm) (Fig. S31–41†). The individual block content ratios determined from the ^{1}H NMR spectra were in good correlation with the calculated values based on the monomer to initiator ratio (Table S4†).

^{1}H NMR spectral analysis of the BAB triblock copolymers **9a–c** (Fig. S37†) indicated high vinyl end-capping efficiency ($f > 80\%$) suggesting that further functionalisation/elaboration could be possible. Therefore the sequential ROMP was quenched with the α-bromoester substituted phenylmethyl ether **E** instead of ethyl vinylether to give the bifunctional triblock PPV macroinitiator **10** in excellent yield with excellent end capping efficiency (95% yield, $f > 87\%$). Under similar ATRP reaction conditions to those in Scheme 1 the macroinitiator **10** and MMA gave coil–rod–rod–rod–coil CBABC pentablock copolymers **11a–c** with molecular weights ranging from 20.6–36.5 kDa and dispersities in the range 1.49–1.25. The slightly broader dispersity of **11a** is due to partial isomerisation of the *cis*-alkenes (Scheme 3, Table S3 and Fig. S28–30†).

Furthermore the sequential ROMP approach can be used to synthesise fully conjugated pentablock copolymers as shown in Scheme 4. Dialkyl monomer **M2** was subjected to ROMP

([**M2**]/[**1**] = 10) in the presence of 3-BrPy ligand and upon complete consumption the dialkoxy monomer **M1** was added and stirred for 15 h, complete consumption of this monomer (**M1**) was followed by addition of either **M2** or a mixture of the isomeric tetraalkyl monomers **M3**, **M4** (**M4** being unreactive). The polymerisation reaction was eventually quenched by adding excess ethylvinyl ether and the fully conjugated ABABA and CBABC type pentablock copolymers **12** and **13** were isolated by precipitation (Scheme 4, S43 & S45†).

Dilute solutions of conjugated polymers **2a–c**, **3a–c**, **8a–c**, **9a–c**, **12** and **13** in degassed anhydrous dichloromethane were subjected to photoisomerisation under UV irradiation at 365 nm for 48–72 h. ^{1}H NMR analysis of the polymers obtained indicated complete isomerisation and an all *trans* geometry of the backbone vinylenes (Fig. 4a, also see ESI†). In the GPC a lower retention time was observed for the all *trans* isomers as expected because of the higher hydrodynamic volume of this polymer (Fig. 4b).

The optical properties of the parent homopolymers were measured in solution (Fig. S49 and Table S5†) and the block copolymers were recorded in both solution and as thin films (Fig. 5, S50–54, and Table S5†). The absorption spectra of the fully conjugated tri and pentablock copolymers **8a–c**, **9a–c**, **12** and **13** showed λ_{max} values around 450 nm and 380 nm correlating to absorptions of the individual blocks **2a–c** and **3a–c**. Increasing the content of monomer **M2** in polymers **8a** to **8c** increased the intensity at 370 nm in direct correlation with the ratio of the individual blocks (Fig. 5a). For polymers **9a–c** the absorption maxima were red shifted going from **9a** to **9c** with
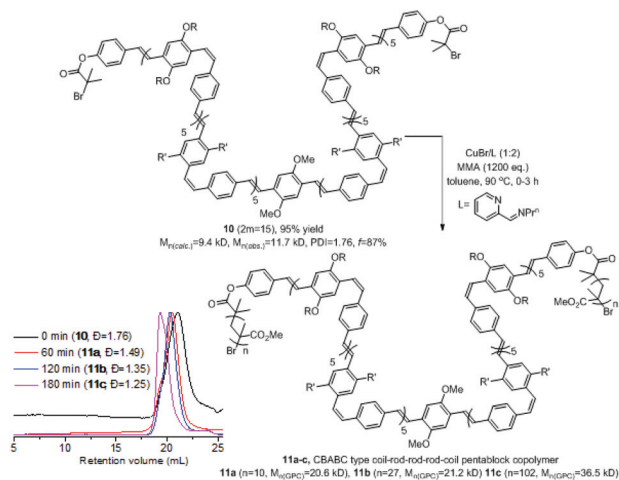
Scheme 3 Sequential ROMP-ATRP strategy to coil–rod–rod–rod–coil CBABC pentablock copolymers **11a–c** (GPC in THF).
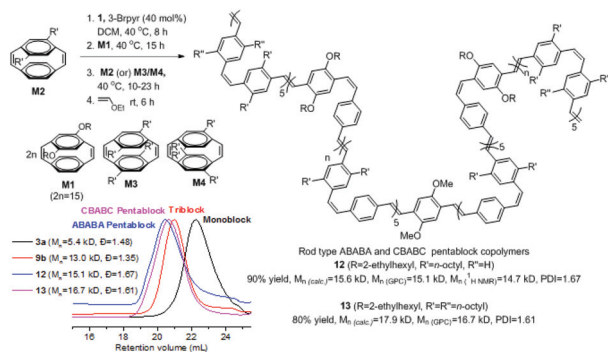
Scheme 4 Sequential ROMP strategy to fully conjugated rod ABABA **12** and CBABC **13** pentablock copolymers (GPC in THF).
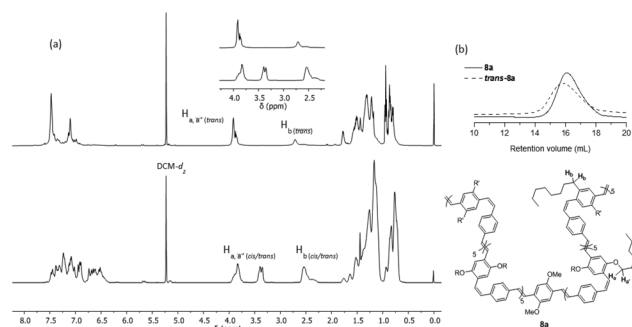

Fig. 4 Photoisomerisation of triblock copolymer **8a**, (a) ^{1}H NMR spectra of **8a** and *trans*-**8a** in DCM-d_2, (b) GPC traces of **8a** and *trans*-**8a** in CHCl₃.
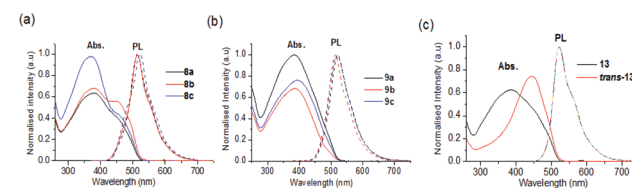

Fig. 5 Absorption and emission profiles of rod (a) ABA triblock (b) BAB triblock and (c) CBABC pentablock copolymers.

increasing alkoxy monomer content (Fig. 5b). Excitation of the block copolymer **8a–c**, **9a–c**, **12** and **13** at 370 nm and the corresponding all *trans* isomers at 440 nm resulted in emission maxima approximately at 520 nm (Table S5†).

The absorption and emission spectra of rod–coil block copolymers **6a–c**, **7a–c** and **11a–c** showed absorption maxima at 460 nm (**6a–c**), 400 nm (**7a–c**), 370 nm (**11a–c**) and emission maxima at 527 nm (**6a–c**), 491 nm (**7a–c**) and 520 nm (**11a–c**). These values agree well with those of parent macroinitiators **4a**, **5a** and **10**, indicating that the PMMA block has no influence on the optical properties of these materials. The Φ_{PL} of the macroinitiators **4a**, **5a** and **10** and the block copolymers **7a–c**, **8a–c** and **11a–c** are identical and this suggests that the radical polymerisation did not perturb the π-conjugated backbone (Table S5†). A small red shift in emission maxima values (~20 nm) was observed in the solid state spectra of the block copolymers consistent with previous studies on PPV polymers (Fig. S53–54 and Table S6†).[28]

The electrochemical properties of the homopolymers (**2a–c** and **3a–c**) and fully conjugated block copolymers (**8a–c**, **9a–c**, **12** and **13**) were studied by cyclic voltammetry in dichloromethane using $[(C_4H_9)_4N]PF_6$ (0.1 M solution in DCM) as the electrolyte in conjunction with a platinum working electrode. The calculated HOMO and LUMO energy levels for **2a–c** are consistent with the reported values (HOMO = −5.14 and LUMO = −2.56 eV) for these polymers.[28] The homopolymers **3a–c** have deeper HOMO levels (~−5.36 eV) (Table 1, entries 1 & 3 and Table S7†).

The HOMO and LUMO energy levels of the tri- and pentablock copolymers are consistent with those of the parent homopolymers. The *cis/trans* ABA triblock BCPs **8a–c** exhibited reversible oxidation $E_{1/2}$ values in the range of 0.6–0.4 V, with slight increase in HOMO energy levels (−5.23 to −5.05 eV) but the BCPs **9a–c** showed the same HOMO value (~−5.14 eV) indi-

cating localisation of the HOMO on the dialkoxyphenylene vinylene block in **9a–c**. The LUMO energy levels for BCPs **8a–c** and **9a–c** are in a similar range, −2.69 to −2.78 eV for **8a–c** and −2.60 to −2.67 eV for **9a–c** (Table S7† and Table 1, entries 5–7 & 9–11). The *cis/trans* pentablock copolymers **12** and **13** showed reversible oxidation and reduction potentials $E_{1/2}$ at 0.5–0.6 V and −1.99, −1.80 V with the HOMO energy level approximately −5.14 eV but slightly deeper LUMO level (−2.79 eV) for BCP **13** (Table S7† and Table 1, entries 13 & 15). In general, the all *trans* homo and block copolymers have a higher lying HOMO when compared to their *cis/trans* forms due to extended conjugation in the *trans* form. Also, a consistent deepening of LUMO levels was observed for all the *trans* polymers except for ***trans*-13** (Table 1, entries 15 & 16). Finally, a clear trend in bandgap reduction was observed for the all *trans* polymers due to extended delocalisation and both the electrochemical and optical bandgap values for all the polymers are comparable (Table 1).

Conclusions

In summary, the first bidirectional ROMP of strained para-cyclophane-1,9-dienes using a bifunctional Hoveyda–Grubbs initiator is reported. This methodology was used in the controlled synthesis of rod–rod and rod–coil tri- and pentablock copolymers through sequential ROMP and ROMP-ATRP reactions. The initially formed *cis,trans* polymers can be photo-isomerised to the corresponding all *trans* forms. The optical properties of the block copolymers directly correlate with those of the individual polymer blocks and complete energy transfer between blocks is observed in the fluorescence emission spectra of thin films. Fluorescence quantum efficiency measurements of the rod–coil block copolymers showed no damage to π-conjugated backbone under radical ATRP reaction conditions.

Conflicts of interest

There are no conflicts to declare.

Acknowledgements

Table 1 Electrochemical properties of homopolymers (**2a** & **3a**) and block copolymers (**8a–c**, **9a–c**, **12** & **13**)

Entry	Polymer	HOMO[a] (eV)	LUMO[b] (eV)	$E_{g(elc)}$[c,d] (eV)
1	**2a**	−5.14	−2.66	2.48 (2.30)
2	**2a (E)**	−5.01	−2.84	2.17 (2.28)
3	**3a**	−5.36	−2.58	2.78 (2.50)
4	**3a (E)**	−5.10	−2.81	2.29 (2.46)
5	**8a**	−5.23	−2.77	2.46 (2.31)
6	**8b**	−5.12	−2.69	2.43 (2.27)
7	**8c**	−5.05	−2.78	2.27 (2.27)
8	**8b (E)**	−5.03	−2.70	2.33 (2.29)
9	**9a**	−5.10	−2.67	2.43 (2.33)
10	**9b**	−5.14	−2.66	2.48 (2.32)
11	**9c**	−5.14	−2.60	2.54 (2.30)
12	**9a (E)**	−5.02	−2.75	2.27 (2.30)
13	**12**	−5.14	−2.64	2.50 (2.34)
14	**12 (E)**	−5.04	−2.69	2.35 (2.29)
15	**13**	−5.19	−2.79	2.40 (2.31)
16	**13 (E)**	−5.05	−2.67	2.38 (2.28)

[a] HOMO = $(E_{ox}^{onset} - Fc_{ox}) + 4.8$. [b] LUMO = $(E_{red}^{onset} - Fc_{ox}) + 4.8$. [c] $E_{g\,(elc.)}$ = HOMO–LUMO. [d] Optical band gap values in parenthesis ($E_{g\,(opt.)}$ = $1240/\lambda_{onset}$).

References

1 A. C. Grimsdale, K. Leok Chan, R. E. Martin, P. G. Jokisz and A. B. Holmes, *Chem. Rev.*, 2009, **109**, 897–1091.

2 L. Dou, Y. Liu, Z. Hong, G. Li and Y. Yang, *Chem. Rev.*, 2015, **115**, 12633–12665.

3 Y. He, W. Hong and Y. Li, *J. Mater. Chem. C*, 2014, **2**, 8651–8661.

4 L. Ying, F. Huang and G. C. Bazan, *Nat. Commun.*, 2017, **8**, 14047.

5 L. Lu, T. Zheng, Q. Wu, A. M. Schneider, D. Zhao and L. Yu, *Chem. Rev.*, 2015, **115**, 12666–12731.

6 D. Khim, G.-S. Ryu, W.-T. Park, H. Kim, M. Lee and Y.-Y. Noh, *Adv. Mater.*, 2016, **28**, 2844–2844.

7 C. Zhang, P. Chen and W. Hu, *Chem. Soc. Rev.*, 2015, **44**, 2087–2107.

8 J. R. Sheats and P. F. Barbara, *Acc. Chem. Res.*, 1999, **32**, 191–192.

9 M. Lee, B.-K. Cho and W.-C. Zin, *Chem. Rev.*, 2001, **101**, 3869–3892.

10 F. Mathias, A. Fokina, K. Landfester, W. Tremel, F. Schmid, K. Char and R. Zentel, *Macromol. Rapid Commun.*, 2015, **36**, 959–983.

11 M. He, F. Qiu and Z. Lin, *J. Mater. Chem.*, 2011, **21**, 17039–17048.

12 S. Miyane, H. Mori and T. Higashihara, *Microsyst. Technol.*, 2016, **22**, 3–10.

13 J. Wang, M. Ueda and T. Higashihara, *ACS Macro Lett.*, 2013, **2**, 506–510.

14 M. Verswyvel, J. Steverlynck, S. Hadj Mohamed, M. Trabelsi, B. Champagne and G. Koeckelberghs, *Macromolecules*, 2014, **47**, 4668–4675.

15 K. B. Woody, B. J. Leever, M. F. Durstock and D. M. Collard, *Macromolecules*, 2011, **44**, 4690–4698.

16 C. W. Bielawski, T. Morita and R. H. Grubbs, *Macromolecules*, 2000, **33**, 678–680.

17 G. Qu, F. Jiang, S. Zhang and S. Usuda, *Mater. Lett.*, 2007, **61**, 3421–3424.

18 H. Wang, W. You, P. Jiang, L. Yu and H. H. Wang, *Chem. – Eur. J.*, 2004, **10**, 986–993.

19 L. zur Borg, A. L. Domanski, R. Berger and R. Zentel, *Macromol. Chem. Phys.*, 2013, **214**, 975–984.

20 C.-Y. Yu and M. L. Turner, *Angew. Chem.*, 2006, **118**, 7961–7964.

21 A. M. Spring, C.-Y. Yu, M. Horie and M. L. Turner, *Chem. Commun.*, 2009, 2676–2678.

22 C.-Y. Yu, M. Helliwell, J. Raftery and M. L. Turner, *Chem. – Eur. J.*, 2011, **17**, 6991–6997.

23 B. J. Lidster, D. R. Kumar, A. M. Spring, C.-Y. Yu and M. L. Turner, *Polym. Chem.*, 2016, **7**, 5544–5551.

24 D. R. Kumar, B. J. Lidster, R. W. Adams and M. L. Turner, *Polym. Chem.*, 2017, **8**, 3186–3194.

25 S.-W. Chang and M. Horie, *Chem. Commun.*, 2015, **5**, 9113–9116.

26 D. Mäker, C. Maier, K. Brödner and U. H. F. Bunz, *ACS Macro Lett.*, 2014, 415–418.

27 F. Menk, M. Mondeshki, D. Dudenko, S. Shin, D. Schollmeyer, O. Ceyhun, T.-L. Choi and R. Zentel, *Macromolecules*, 2015, **48**, 7435–7445.

28 C.-Y. Yu, M. Horie, A. M. Spring, K. Tremel and M. L. Turner, *Macromolecules*, 2009, **43**, 222–232.

29 C. Y. Yu, J. W. Kingsley, D. G. Lidzey and M. L. Turner, *Macromol. Rapid Commun.*, 2009, **30**, 1889–1892.

30 F. Menk, S. Shin, K.-O. Kim, M. Scherer, D. Gehrig, F. Laquai, T.-L. Choi and R. Zentel, *Macromolecules*, 2016, **49**, 2085–2095.

31 E. Elacqua, G. T. Geberth, D. A. Vanden Bout and M. Weck, *Chem. Sci.*, 2019, **10**, 2144–2152.

32 S. K. Pomarico, D. S. Lye, E. Elacqua and M. Weck, *Polym. Chem.*, 2018, **9**, 5655–5659.

33 B. J. Lidster, J. M. Behrendt and M. L. Turner, *Chem. Commun.*, 2014, **50**, 11867–11870.

34 I. Cosemans, J. Vandenbergh, L. Lutsen, D. Vanderzande and T. Junkers, *Polym. Chem.*, 2013, **4**, 3471–3479.

35 K. Nomura, T. Haque, T. Onuma, F. Hajjaj, M. S. Asano and A. Inagaki, *Macromolecules*, 2013, **46**, 9563–9574.

36 G. Tu, H. Li, M. Forster, R. Heiderhoff, L. J. Balk and U. Scherf, *Macromolecules*, 2006, **39**, 4327–4331.

37 H. Wang, H. H. Wang, V. S. Urban, K. C. Littrell, P. Thiyagarajan and L. Yu, *J. Am. Chem. Soc.*, 2000, **122**, 6855–6861.

38 F. He, T. Gädt, M. Jones, G. D. Scholes, I. Manners and M. A. Winnik, *Macromolecules*, 2009, **42**, 7953–7960.

39 P. Lu, N. M. Alrashdi and A. J. Boydston, *J. Polym. Sci., Part A: Polym. Chem.*, 2017, **55**, 2977–2982.

40 B. J. Lidster, D. R. Kumar, A. M. Spring, C.-Y. Yu, M. Helliwell, J. Raftery and M. L. Turner, *Org. Biomol. Chem.*, 2016, **14**, 6079–6087.

41 K. Grudzień, M. Malinska and M. Barbasiewicz, *Organometallics*, 2012, **31**, 3636–3646.

42 R. A. Segalman, B. McCulloch, S. Kirmayer and J. J. Urban, *Macromolecules*, 2009, **42**, 9205–9216.

43 N. Sary, L. Rubatat, C. Brochon, G. Hadziioannou, J. Ruokolainen and R. Mezzenga, *Macromolecules*, 2007, **40**, 6990–6997.

44 It is common that the M_n values obtained from GPC do not correlate with MALDI-TOF-MS data especially for polydisperse polymers, see: H. Rashidzadeh and B. Guo, *Anal. Chem.*, 1998, **70**, 131–135.